J Physiol 588.11 (2010) pp 1829–1840

TOPICAL REVIEW

Axon initial segment dysfunction in epilepsy

Verena C. Wimmer[1], Christopher A. Reid[1,3], Eva Y.-W. So[1], Samuel F. Berkovic[2] and Steven Petrou[1,3]

[1]*Florey Neuroscience Institutes, University of Melbourne, Parkville 3052, Victoria, Australia*
[2]*Epilepsy Research Centre, University of Melbourne (Austin Health), Heidelberg West 3081, Victoria, Australia*
[3]*Centre for Neuroscience, University of Melbourne, Parkville 3052, Victoria, Australia*

The axon initial segment (AIS) contains the site of action potential initiation and plays a major role in neuronal excitability. AIS function relies on high concentrations of different ion channels and complex regulatory mechanisms that orchestrate molecular microarchitecture. We review recent evidence that a large number of ion channels associated with epilepsy are enriched at the AIS, making it a 'hotspot' for epileptogenesis. Furthermore, we present novel data on the clustering of GABRγ2 receptors in the AIS of cortical and hippocampal neurons in a knock in mouse model of a human genetic epilepsy. This article highlights the molecular coincidence of epilepsy mutations at the AIS and reviews pathogenic mechanisms converging at the AIS.

(Received 9 February 2010; accepted after revision 30 March 2010; first published online 7 April 2010)
Corresponding author S. Petrou: Florey Neuroscience Institutes, Parkville, Victoria 3010, Australia; The University of Melbourne, Parkville 3010, Australia. Email: spetrou@unimelb.edu.au

Abbreviations AAV, adenoassociated virus; AIS, axon initial segment; AP, action potential; AnkG, ankyrinG; BFNIS, benign familial neonatal-infantile seizures; BFNS, benign familial neonatal seizures; CAE, childhood absence epilepsy; CAMs, cellular adhesion molecules; FS, febrile seizures; $GABA_AR$, $GABA_A$ receptor; GEFS+, genetic (generalised) epilepsy with febrile seizures plus; GAERS, generalised absence epilepsy rats from Strasbourg; IGE, idiopathic generalised epilepsy; MAGUK, membrane-associated guanylate kinase family; S1, primary somatosensory cortex.

Axon initial segment: functional relevance and connection with epilepsy

Information processing in neurons relies on the integration of excitatory and inhibitory inputs to make a yes-or-no decision to fire an action potential (AP). In most neurons this processing occurs at the axon initial segment (AIS), a specialised domain of the axon proximal to the soma (Fig. 1). Once regarded simply as a point of AP initiation, there is now growing evidence of both functional and structural complexity of this specialised neuronal compartment (Ogawa & Rasband, 2008; Song *et al.* 2009). For example, it has only been recently recognised that different neuronal subtypes possess AISs with unique properties and forms of plasticity (Goldberg *et al.* 2008; Hu *et al.* 2009). AIS function is dependent on high density clustering of a multitude of different ion channels. Intriguingly, a significant number of these channels have been associated with human epilepsy, in particular Na^+ channel subunits, $GABA_A$ receptors, K^+ channels and Ca^{2+} channels. This paper will review our growing understanding of epilepsy-associated proteins localised at the AIS. We propose that the AIS represents one 'common pathogenic node' in epilepsy, where independent molecular mechanisms cause similar effects on neuronal function by altering the properties of AIS-mediated signal transmission leading to hyper-synchronous neuronal behaviour.

Verena Wimmer and Steven Petrou are from the Florey Neuroscience Institutes in Melbourne, Australia. Dr Wimmer undertook PhD and post-doctoral studies at the Max Planck Institute for Medical Research in Heidelberg with Bert Sakmann and Thomas Kuner and subsequently began her studies in genetic epilepsies combining quantitative imaging approaches with *in vivo* delivery of virally expressed genes and reporters. Dr Petrou heads a team of multidisciplinary researchers aimed at revealing the disease mechanism of genetic epilepsy and has held a long term interest in ion channels and in particular their involvement in pathogenesis of human disease.

DOI: 10.1113/jphysiol.2010.188417

The AIS – a specialised region of the axon

Evidence for AP initiation at the AIS first appeared in the 1950s. Classical experiments, using antidromic and orthodromic stimulation in motor neurons, revealed that the AIS spike always preceded the somatic spike (Araki & Otani, 1955; Coombs *et al.* 1957; Fatt, 1957). An early computer model by Dodge & Cooley (1973) predicted that a high local density of Na^+ channels in the AIS, as in the nodes of Ranvier, would lower the threshold membrane potential for AP initiation in the AIS (Dodge & Cooley, 1973). Indeed, cytochemical and electron microscopic freeze fracture studies previously identified membrane similarities between the AIS and the nodes suggesting that Na^+ channel density would be likewise similar (Palay *et al.* 1968; Rosenbluth, 1976; Waxman & Quick, 1978).

Molecular composition of the AIS

The molecular and structural architecture of the AIS is defined by a specialised and complex cytomatrix. The large scaffolding protein ankyrinG (AnkG) is critical for assembly of AIS components and is frequently used as the defining molecular marker of this structure. AnkG itself is attached to βIV spectrin, which, in turn, anchors the whole submembrane scaffold to the actin cytoskeleton. High concentrations of cellular adhesion molecules (CAMs), including Caspr2, Nf-186 and NrCAM, are also found at the AIS and are thought to be involved in establishing a specialised extracellular matrix that surrounds the AIS (Hedstrom *et al.* 2007).

The AIS cytomatrix is geared to supporting and modulating the ion channels responsible for generating APs. For example, Na^+ and KCNQ channels bind directly to AnkG while Kv1 channels are anchored at the AIS via PSD-93, a member of the PDZ-domain containing membrane-associated guanylate kinase family (MAGUK; Ogawa & Rasband, 2008). It is the ability of the AIS to maintain these voltage-sensitive channels at high densities that makes it the point of AP initiation within the neuron.

The three major brain Na^+ channel α-subunits, $Na_v1.1$, $Na_v1.2$ and $Na_v1.6$, and the $\beta1$ accessory subunit are all enriched in the AIS (Van Wart *et al.* 2007; Duflocq *et al.* 2008; Kole *et al.* 2008; Lorincz & Nusser, 2008; Brackenbury *et al.* 2010). AP waveform properties are further influenced by K^+ channels residing at the AIS, and to date, Kv1.1/2/4 and KCNQ2/3 have all been identified at the AIS (Chung *et al.* 2006; Inda *et al.* 2006; Van Wart *et al.* 2007; Sarmiere *et al.* 2008; Shah *et al.* 2008). More recently, R- and T-type Ca^{2+} channels have also been found at the AIS (Bender & Trussell, 2009). Mutations with functional changes in these AIS channels or structural proteins are a highly plausible mechanism of epileptogenesis by affecting the excitability of neurons and networks.

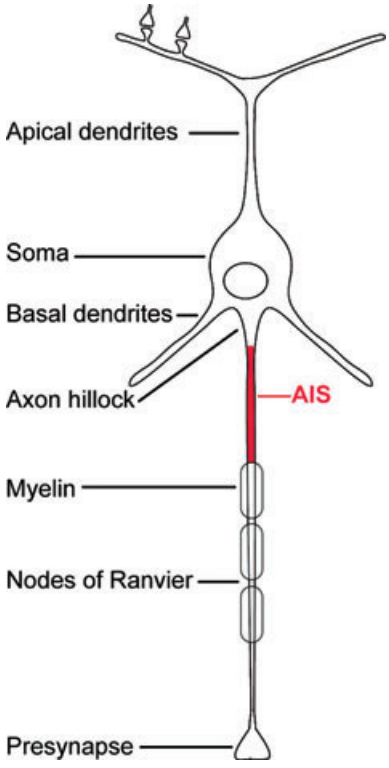

Figure 1. Neuronal anatomy, axonal compartments and the AIS
The AIS (highlighted in red) includes the first 30–70 μm – depending on the cell type – of axon adjacent to the axon hillock.

Measuring AIS function

The morphology of the AIS and the molecular arrangement of ion channels and anchoring proteins determine the functional properties of the AIS. APs are thought to be initiated when the distal end of the AIS is sufficiently depolarised. The spike then propagates back to the cell body, where the somatic component of the AP is generated, which presumably contributes to back-propagation of APs. The temporal sequence of these events imparts a characteristic signature on the AP shape as recorded using current clamp (Fig. 2). Functional details about AP initiation can then be derived by simply calculating the first and second derivatives of the AP voltage trace (dV/dt and d^2V/dt^2; Fig. 2).

Direct cell-attached whole-cell recordings have revealed the specific contributions of AIS channels to AIS function. $Na_v1.6$ contributes to AP initiation and $Na_v1.2$ to AP backpropagation, K^+ channels modify AP waveform and Ca^{2+} channels underlie and shape AP bursts (Kole *et al.* 2007; Bender & Trussell, 2009; Hu *et al.* 2009). Single-cell voltage sensitive dye imaging from axonal compartments has provided insight into tempero-spatial dynamics of AP initiation in the distal AIS and orthodromic and antidromic propagation of the spike (Palmer & Stuart, 2006).

To fully appreciate the potential for AIS dysfunction in epilepsy we next detail the current state of knowledge of epilepsy associated mutations in AIS resident ion channels and how they may change excitability.

Na^+ channels

Given the role of Na^+ channels in AP initiation, it is not surprising that most mutations associated with epilepsy have been found in genes coding for these channels, in particular the α-subunit genes *SCN1A, SCN2A* and the accessory β-subunit gene *SCN1B*.

SCN1A/Na_V1.1. Mutations in *SCN1A* cause epilepsies of varying severity within the phenotypic spectrum known as genetic (generalised) epilepsy with febrile seizures plus (GEFS+; Scheffer *et al.* 2007, 2009). This diversity is thought to be correlated with the particular type of mutation involved, i.e. mutations with subtle functional effects tend to cause mild phenotypes such as benign febrile seizures (FS). In contrast, complete loss-of-function mutations lead to Dravet's syndrome, a severe encephalopathy. Mice with heterozygous *Scn1a* loss-of-function mutations have been used as rodent models for human Dravet's syndrome (Yu *et al.* 2006; Ogiwara *et al.* 2007) and point to a specific interneuron dysfunction in seizure generation.

Only recently has detailed information about the neuron type expression and the subcellular localisation of Na_V1.1 become available (Duflocq *et al.* 2008; Lorincz & Nusser, 2008) and it has been shown that Na_V1.1 appears to be localised exclusively to interneuron AISs (Fig. 3). Taken together, these two lines of evidence suggest that Dravet's syndrome may be caused by a specific deficit in the function of interneuron AISs. However, further functional studies are required to test this hypothesis.

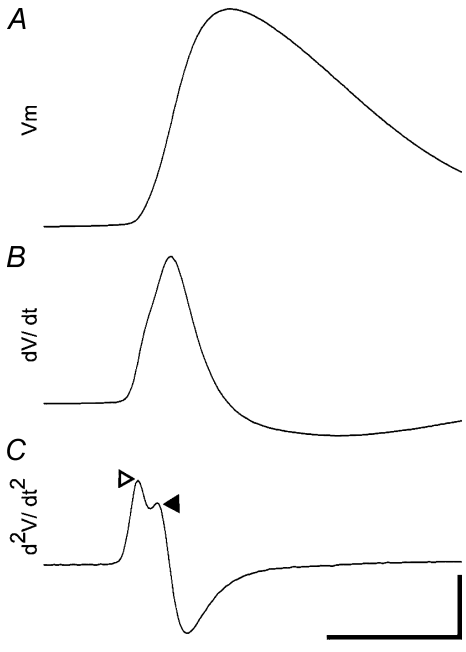

Figure 2. AIS function in acute brain slices can be analysed using somatic patch clamp recordings
A, averaged AP waveform. *B*, time-aligned fist derivative of AP waveform (dV/dt). *C*, time-aligned second derivative (d^2V/dt^2). Characteristic signature of sequential AP initiation in the AIS (open arrowhead) and soma (filled arrowhead). Time bar 1 ms, V_m bar 20 mV (*A*), dV/dt bar 100 mV s^{-1} (*B*), and d^2V/dt^2 bar 1000 mV s^{-2} (*C*).

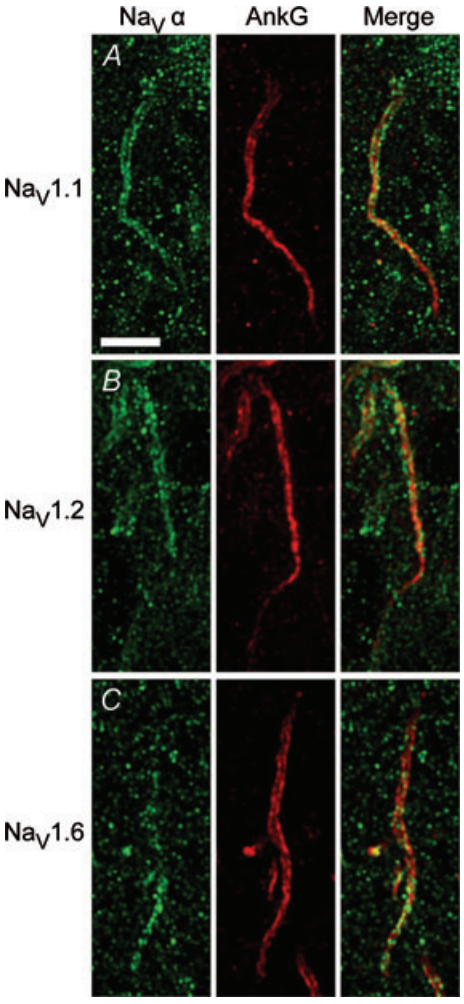

Figure 3. Three major Na^+ channel α-subunits localise to the AIS
Our own immunohistochemical stainings reproduced the interneuron-specificity of Na_V 1.1 expression suggested by Lorincz & Nusser (2008) (but also see Duflocq *et al.* 2008) as well as gradient distribution of Na_V1.2 and Na_V1.6. Green: staining against Na^+ channel α-subunit, red: staining against AnkG. *A*, inhibitory interneuron-specific expression of Na_V1.1 in proximal half of the AIS (inhibitory neuron in stratum radiatum in hippocampus). *B*, in adult mice Na_V1.2 is concentrated in the proximal half of pyramidal cell AIS (CA3). *C*, Na_V1.6 gradient with peak concentration in distal AIS (CA3). Scale bar 5 μm.

***SCN2A*/$Na_V1.2$.** Missense mutations of *SCN2A* cause benign familial neonatal-infantile seizures (BFNIS), a relatively mild form of childhood epilepsy that usually resolves within the first year of life (Berkovic *et al.* 2004). Cell biological studies show that this neonatal seizure onset corresponds well to the specific expression pattern of $Na_V1.2$. During embryonic and early postnatal development $Na_V1.2$ is the main Na^+ channel in the AIS of excitatory neurons but $Na_V1.6$ expression increases soon after birth (Fig. 3). In adult animals the two Na^+ channel α-subunits show complementary localisation gradients within the AIS with $Na_V1.2$ occupying the proximal half of the AIS and $Na_V1.6$ being concentrated in the distal half (Fig. 3; Boiko *et al.* 2003). These observations imply that mutations in *SCN2A* may have their biggest effect on AIS function in infants (Xu *et al.* 2007) while the increase in $Na_V1.6$ expression may be able to compensate for these deficits later in life. More severe mutations in *SCN2A* may cause refractory seizures beginning in early childhood (Ogiwara *et al.* 2009).

FS is the commonest childhood seizure syndrome. They are sometimes due to monogenic missense mutations in *SCN1A* or *GABRG2* (Wallace *et al.* 1998; Wallace *et al.* 2001), but more commonly have a complex genetic architecture due to multiple and, as yet, unidentified genes. A potential common pathway may involve a $Na_V1.2$ mediated AIS mechanism. Work in our laboratory investigating wild-type $Na_V1.2$ channels showed that their voltage dependence of activation was exquisitely sensitive to physiological changes in temperature. A febrile increase in recording temperature, from 37°C to 41°C, produced an 8 mV left-shift in half-activation voltage that would result in the direct temperature-dependent opening of AIS localised $Na_V1.2$ channels. Computational modelling showed that this change in activation voltage could readily produce epileptiform network activity (Thomas *et al.* 2009).

***SCN8A*/$Na_V1.6$.** Only one mutation in the gene for human $Na_V1.6$ channels has been found to date; this heterozygous null mutation leads to cerebellar atrophy, ataxia and mental retardation but an epileptic phenotype was not seen (Trudeau *et al.* 2006). However, there is a wealth of evidence from animal studies that connects $Na_V1.6$ with epilepsy (Papale *et al.* 2009) and suggests a major role for $Na_V1.6$ in AP initiation at the AIS (Royeck *et al.* 2008). Patch clamp and modelling studies on neurons from *Scn8a* knock out mice show impaired AP firing (Van Wart *et al.* 2007; Royeck *et al.* 2008). Furthermore, it has been proposed that $Na_V1.2$ and $Na_V1.6$ serve distinct, subtype specific functions in AP initiation with $Na_V1.6$ being responsible for AP initiation at the distal end of the AIS and $Na_V1.2$ mediating AP backpropagation to the soma (Hu *et al.* 2009). Heterogeneity of AIS Na^+ channel distribution in different neuron types would be an important determinant of neuronal excitability in normal function as well as in pathological states such as epilepsy. For example, a more proximal spike initiation zone significantly reduces cellular excitability (Kress *et al.* 2010).

The critical role of $Na_V1.6$ in neuronal output is illustrated by reduced susceptibility to experimentally induced seizures not only in heterozygous *Scn8a* knock out mice but also in a *Scn1a*/*Scn8a* double knock out mouse strain (Martin *et al.* 2007; Blumenfeld *et al.* 2009). *Scn1a* heterozygous knock out mice model Dravet's syndrome, a severe form of childhood epilepsy. In the *Scn1a*/*Scn8a* double knock out, seizure severity was dramatically reduced (Martin *et al.* 2007), indicating a protective antagonistic epistatic mechanism probably relating to inhibition of AP initiation in the distal AIS. Interestingly, however, *Scn8a* knock out mice and mice carrying a $Na_V1.6$ missense mutation show absence epilepsy, suggesting brain region specific effects of genetic manipulation of this Na^+ channel subunit (Papale *et al.* 2009).

Mutations in *SCN9A* have also been shown to be associated with FS (Singh *et al.* 2009) but there is no direct evidence that $Na_V1.7$ is localised to the AIS although it is clearly axonal (Rush *et al.* 2005).

***SCN1B*/β1.** Functional properties of Na^+ channel α-subunits are modulated by accessory β-subunits. β1 (*SCN1B*) mutations have been found in patients with GEFS+ and Dravet's syndrome (Wallace *et al.* 1998; Scheffer *et al.* 2007; Patino *et al.* 2009). Wild-type β1 has been found in nodes of Ranvier and has recently been shown to also reside in the AIS (Brackenbury *et al.* 2010), which itself has been postulated to be a specialised nodal compartment (Hill *et al.* 2008). Experiments in *Scn1b* knock out mice showed that cerebellar granule neurons lacking β1 were hypoexcitable due to a reduction in resurgent Na^+ current, suggesting that β1 is required for high-frequency firing in these neurons (Brackenbury *et al.* 2010). The precise role of β1 in other neuron types and how epilepsy mutations modulate this function is yet to be determined.

$GABA_A$ receptors

$GABA_A$ receptors (GABRs) mediate inhibition in the brain and mutations resulting in decreased $GABA_AR$ function have been shown to cause neuronal hyperexcitability and epilepsy (Tan *et al.* 2007). AIS targeting of different $GABA_AR$ subunits has been known for more than a decade (Nusser *et al.* 1995; Christie & De Blas, 2003), but our novel data now suggest a direct effect of human $GABA_AR$ mutations on axo-axonic inhibition (see below). This type of inhibition, which is predominantly mediated by

a specific interneuron subclass (Chandelier or axo-axonic neurons), plays an important role in synchronisation of large ensembles of excitatory neurons (Cardin *et al.* 2009). Deficits in axo-axonic inhibition have also been implicated in epilepsy (Howard *et al.* 2005).

$GABA_AR$ $\gamma2$. Several mutations in the $\gamma2$-subunit of GABRs have been associated with FS, GEFS+ and childhood absence epilepsy (CAE; Baulac *et al.* 2001; Wallace *et al.* 2001). Local field potential and EEG recordings in rodent models of these different phenotypes suggest involvement of different brain regions in seizure generation; early epileptiform activity during FS is detected in the hippocampus followed by generalisation of FS involving cortical structures (Dube *et al.* 2007; Oakley *et al.* 2009) whereas absence seizures require participation of a thalamocortical loop (Kostopoulos, 2001).

Differential $GABA_AR$ $\gamma2$ expression at hippocampal and cortical AISs. Interestingly, one mutation, $\gamma2$(R43Q), can cause both seizure types within a given individual, although the mechanism underlying this clinical heterogeneity is unclear. The R43Q mutation, found in a large family with FS and CAE (Wallace *et al.* 2001), has been shown to alter receptor properties (Bianchi *et al.* 2002; Bowser *et al.* 2002; Goldschen-Ohm *et al.* 2010) and trafficking *in vitro* (Frugier *et al.* 2007). Because earlier studies have suggested that $\gamma2$ can cluster at axo-axonic synapse in the AIS (Christie & De Blas, 2003) we investigated the distribution of wild-type and Q43 subunits using immunohistochemical staining. In the CA3 region of the hippocampus, immunohistochemical staining against $\gamma2$ revealed inhibitory postsynapses on somatodendritic compartments and also very high densities of $\gamma2$ positive clusters in AISs (Fig. 4*A* and *D*; 18.7 ± 1.1 $\gamma2$ positive clusters per 10 μm of AIS, $n = 21$ AISs from 2 mice). In comparison, the density of $\gamma2$ containing inhibitory AIS synapses in CA1 and primary somatosensory cortex (S1) is much lower (Fig. 4*B–D*; CA1: 6.6 ± 0.7 $\gamma2$ positive clusters per 10 μm of AIS, $n = 26$ AISs from 2 mice; S1: 5.4 ± 0.5 $\gamma2$ positive clusters per 10 μm of AIS, $n = 40$ AISs from 2 mice; ANOVA; $P < 0.0001$; L2/3 and L5 were pooled because the number of $\gamma2$ positive clusters per 10 μm of AIS did not differ between them), suggesting a brain region specific role of $\gamma2$ in axo-axonic inhibition.

Impact of R43Q mutation on $GABA_AR$ $\gamma2$ at hippocampal AIS. We next compared the number of $\gamma2$ positive synapses on the AIS of CA1 neurons in wild-type mice and heterozygous knock in R43Q mice that recapitulate the human epilepsy phenotype (Fig. 4*E*; Tan *et al.* 2007). There were no differences in the number of $\gamma2$ synapses per 10 μm AIS length between genotypes (wild-type: 6.8 ± 0.5, $n = 63$ AISs from 4 mice; RQ: 7.0 ± 0.4, $n = 136$ AISs from 6 mice; *t* test, $P = 0.7067$), indicating that the R43Q mutation does not alter the absolute number of axo-axonic synapses, although we could not exclude the possibility that the intensity of individual synapses would be reduced. Such a reduction would also be consistent with the presumed trafficking deficit of the Q43 subunit. Although earlier *in vitro* work suggests reduced trafficking (Kang & Macdonald, 2004; Frugier *et al.* 2007), it is important to assess whether this occurs *in vivo* and to what extent.

To study $\gamma2$(Q43) subunit trafficking we used viral expression of EGFP-tagged $\gamma2$ wild-type and mutant

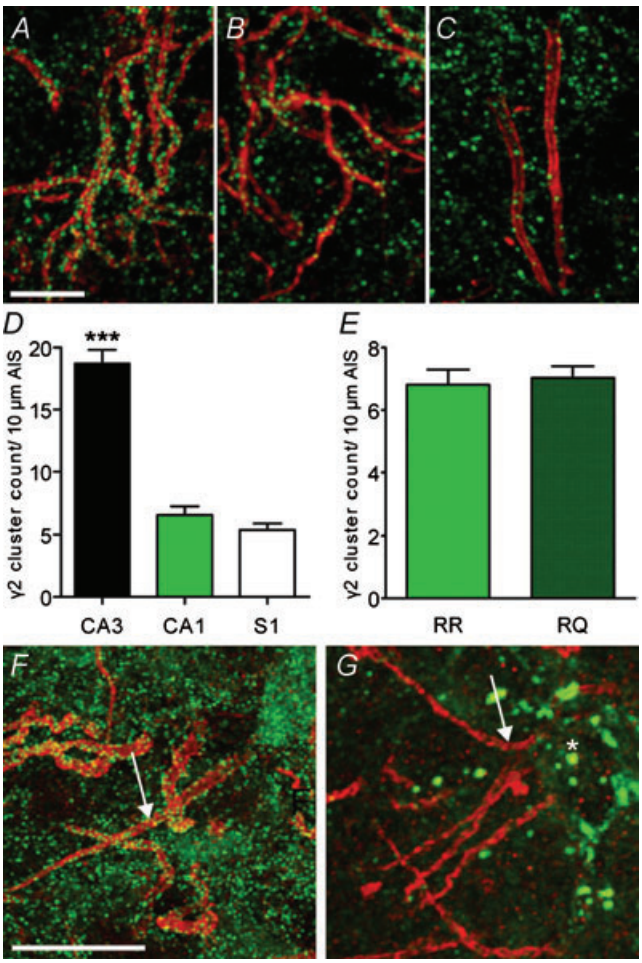

Figure 4. Brain region specific distribution of $\gamma2$
A–E, antibody staining against $\gamma2$ (green) and AnkG (red) in wild-type tissue. *A*, CA3 AISs with high $\gamma2$ cluster densities. *B*, fewer $\gamma2$ clusters in CA1 compared to CA3. *C*, sparse $\gamma2$ clusters in S1 AIS. *D*, difference in the number of $\gamma2$ clusters per 10 μm length of AIS for CA3, CA1 and S1. *E*, no difference in numbers of $\gamma2$ positive postsynapses in wild-type (RR) and heterozygous mutant (RQ) CA1 neurons. *F*, virus-mediated expression of EGFP-$\gamma2$(wild-type) in CA3 neurons. *G*, virus-mediated expression of EGFP-$\gamma2$(Q43) in CA3 neurons. No $\gamma2$ containing clusters were detected. Note accumulation of EGFP-$\gamma2$(Q43) in intracellular compartments (asterisk). Scale bars 10 μm.

subunits *in vivo* in hippocampal CA3 neurons (Fig. 4*F* and *G*). As expected and as we found with our immunohistochemical studies above, EGFP-γ2 wild-type subunits were targeted to somatodendritic and AIS inhibitory synapses (Fig. 4*E*). Such clusters could not, however, be detected in neurons expressing EGFP-γ2(Q43) (Fig. 4*F*; results in CA1 and S1 are identical, data not shown), confirming that the mutation indeed leads to impaired intracellular trafficking and retention of the Q43 subunit (Kang & Macdonald, 2004; Frugier *et al.* 2007) and importantly, showing exclusion of the Q43 subunit from postsynaptic $GABA_A$ receptor clusters in the AIS. We could not quantify differences in γ2 cluster intensity using immunohistochemical staining as the expected changes, ∼35% (Tan *et al.* 2007), would be below the detection limit of antibody methods.

Overall, our results suggest that γ2 clusters are enriched in the AIS of hippocampal CA3 neurons compared to CA1 and S1 neurons and that the Q43 mutation does not alter the number of γ2 containing axo-axonic clusters but rather would cause a reduction in the amount of γ2 per individual cluster. Furthermore, the paucity of γ2 containing clusters in CA1 and S1 compared to CA3 AISs suggests that the R43Q mutation may differentially affect CA3 *versus* CA1 and cortical axo-axonic-inhibition. It is unclear whether such changes would result in reduced inhibition or increased excitation of the AIS, as it has been suggested that the GABA mediated axo-axonic inhibition may be excitatory (Szabadics *et al.* 2006; Khirug *et al.* 2008; Molnar *et al.* 2008; Stafstrom, 2009*b*) or inhibitory (Glickfeld *et al.* 2009). This observation raises the intriguing possibility that the presumed CA3 AIS defect in R43Q patients would give rise to the FS phenotype and that the cortical impact of the R43Q mutation is via a non-AIS mechanism that gives rise to the CAE phenotype. While this remains to be confirmed experimentally, it does provide a molecular explanation for the observed clinical heterogeneity.

Other AIS ion channels associated with epilepsy

K^+ channels. Members of the KCNQ and Kv voltage gated K^+ channels have been found at the AIS (Chung *et al.* 2006; Van Wart *et al.* 2007; Ogawa & Rasband, 2008; Sarmiere *et al.* 2008; Shah *et al.* 2008). Human mutations in Kv1.1 and KCNQ2/3 have been reported and clinical phenotypes are episodic ataxia (EA1) and benign familial neonatal seizures (BFNS), respectively (Browne *et al.* 1994; Jentsch, 2000; Chung *et al.* 2006; Miceli *et al.* 2009). Knock out mouse models of *Kcn1a* and *Kcn2a* both display spontaneous seizures (Smart *et al.* 1998; Brew *et al.* 2007). KCNQ channels (or M channels) modulate the subthreshold membrane potential and dampen excitability of the AIS (Goldberg *et al.* 2008). Interestingly, several human BFNS mutations reduced surface expression of KCNQ channels at the AIS, indicating that reduction in AIS M-current plays a role in the pathophysiology of BFNS (Chung *et al.* 2006).

Kv channels, on the other hand, are important modulators of AP firing frequency (Goldberg *et al.* 2008; Johnston *et al.* 2008). Kv1.1 channels at the AIS control AP waveform and synaptic efficiency and epilepsy mutations in this channel type may modulate cellular excitability by shortening or broadening of axonal APs, leading to increased frequency and fidelity of AP firing or enhanced synaptic transmission by prolonging Ca^{2+} influx through voltage-gated Ca^{2+} channels, respectively (Kole *et al.* 2007). Once again, functional experiments will be necessary to investigate whether human epilepsies with K^+ channel mutations result from dysfunction of the AIS.

Ca^{2+} channels. The presence of Ca^{2+} channels at the AIS has only recently been shown, and functional characterisation indicates that R- and T-type Ca^{2+} channels reside in the proximal half of the AIS (Bender & Trussell, 2009). Mutations located in CACNA1H that encodes the T-type $Ca_V3.2$ subunit have been found in various forms of idiopathic generalised epilepsy (IGE), including those with absence seizures (Chen *et al.* 2003; Heron *et al.* 2004; Khosravani *et al.* 2004; Khosravani *et al.* 2005; Vitko *et al.* 2005; Heron *et al.* 2007). Most of the human variants tested are predicted to increase Ca^{2+} influx (Heron *et al.* 2007). Given the proposed function of AIS Ca^{2+} channels, which is to generate and shape AP bursts, it is interesting to hypothesise that mutations in the gene for $Ca_V3.2$ may modulate neuronal bursting in patients (Bender & Trussell, 2009). Additional evidence from the generalised absence epilepsy rats from Strasbourg (GAERS) model suggests that gain-of-function mutations in this channel are, in part, responsible for expression of the absence phenotype (Powell *et al.* 2009).

Epilepsy-associated non-ion channel proteins in the AIS

Since the discovery of the first genetic epilepsy mutation in 1995 most of the genes implicated in idiopathic epilepsies involve ion channel subunits and, thus, the general disease mechanism of epilepsy has been conceptualised as that of a 'channelopathy'. However, examples of non-ion channel mutations in epilepsy are challenging this view. One such example stems from the observation that a mutation in an AIS cell adhesion molecule protein is also associated with an epilepsy syndrome (Strauss *et al.* 2006). A human homozygous single base pair deletion in the gene coding for the CAM Caspr2 leads to focal (largely temporal lobe) seizures and intellectual impairment.

More evidence for brain pathogenic mechanisms involving structural AIS proteins is available from animal

models. 'Quivering' mice lacking functional βIV spectrin implicate reduced AIS clustering of Na^+ channel and consequently, reduced excitability of affected neurons (Winkels *et al.* 2009). In addition, proteolysis in response to neuronal injury has been shown to specifically affect the structural integrity of the AIS (Schafer *et al.* 2009). Previously it has been suggested that the cytoskeletal scaffolds rather than ion channel expression may confer both specificity and functional flexibility to the AIS (Ogawa & Rasband, 2008). It is likely that in the coming years a wealth of mutations of AIS structural proteins will appear and that they will exert their epileptogenic action by changing ion channel clustering, targeting and function.

Conclusion

Given the accumulation of epilepsy-associated proteins in the AIS in combination with its role in AP firing, we anticipate it will likewise play a major role in AP firing dysfunction in epileptogenesis. So far, however, the evidence linking AIS dysfunction and epileptic phenotype is largely indirect and further cell-biological and functional experiments that specifically interrogate AIS function in the context of epileptogenesis will be needed to further our understanding of the disease process.

It has been proposed that different epilepsy mutations might share 'points of convergence' in the disease process, i.e. pathogenic mechanisms that are not closely related but independently cause similar effects on neuronal function by altering a particular property of signal transmission, in this case the function of the AIS. Therefore, it can be speculated that the AIS represents a 'structure of convergence', whose properties are altered by epilepsy mutations (Table 1).

The epilepsies include numerous clinical syndromes with hundreds of known human epilepsy mutations and it is almost impossible to imagine specific therapeutic approaches to each of these conditions. In contrast, pathogenic mechanisms converging at the AIS are likely to affect one or a combination of three basic AP properties, AP frequency, waveform and threshold of initiation, all of which are controlled by AIS ion channels and directly translate into neuronal network excitability. Hence, the AIS might provide an excellent target for antiepileptic drugs in the future because multiple AIS related disease mechanisms can be 'reduced' to a few common disease pathways or 'AISopathies'. Not all epilepsies, of course, will be due to AIS dysfunction but similar points of functional convergence may be identified in other epilepsies that promise to tame the potential number of mechanisms predicted by the emerging genetic architecture.

It is curious that AIS proteins have also been associated with other brain disorders, for example the *ANK3* gene coding for AnkG has been identified as a susceptibility locus for bipolar disease (Ferreira *et al.* 2008). These results prompt the question, 'how do mutations affecting the AIS specifically cause either epilepsy or bipolar disease?' They also highlight the bigger issue of co-morbidities associated with epilepsy mutations, e.g. cognitive impairment, intellectual disability, depression, etc. A full understanding of the heterogeneity of AIS molecular anatomy and function across neuron types and brain regions will shed light on these important issues and may point the way forward for novel disease-specific therapeutic interventions.

Methods

Electrophysiology. Experiments were carried out according to the guidelines laid down by the Florey Neuroscience Insititutes' animal welfare committee. P14–16 wild-type mice were anaesthetised with 2% isoflurane before decapitation. The brain was removed and 300 μm sagittal vibrating microtome sections were prepared in a saline ice bath. Slices were allowed to recover at room temperature for 1 h in artificial cerebrospinal fluid (aCSF; in mM: NaCl 125, $NaHCO_2$ 25, KCl 5, NaH_2PO_4 1.25, glucose 10, $MgCl_2$ 1, $CaCl_2$ 2) bubbled with 95% O_2–5% CO_2.

For current clamp recordings, brain slices were perfused with oxygenated aCSF at 34°C. Pyramidal neurons in the subiculum were visualised and identified with IR-DIC microscopy. Somatic whole-cell current-clamp recordings were made with a patch-clamp amplifier (MultiClamp 700A, MDS) using 3–6 MΩ filamented borosilicate micropipettes (GC150F-10, Harvard Instruments) filled with the following solution (in mM): potassium gluconate 125, KCl 5, $MgCl_2$ 2, Hepes 10, ATP-Mg 4, GTP-Na_2 0.3, Tris-phosphocreatine 10, EGTA 10 (pH 7.2, osmolarity 290 mosmol l^{-1}). Standard capacitance compensation and bridge balance techniques were employed. Membrane resistance was between 50–100 MΩ for all recordings.

Ten minutes after break-in, pCLAMP (Molecular Devices, Sunyvale, CA, USA) was used to drive a current-clamp protocol consisting of 20 current steps of 400 ms duration (20 pA incremental steps from −100 pA to 280 pA) with 300 ms baseline recording on either side of the step. A gap of 500 ms was allowed between each sweep. Sampling rate was ∼83 kHz.

Data analysis. Electrophysiological recordings were analysed using custom software written in MATLAB (The Mathworks, Inc., Natick, MA, USA). AP baselines were taken from a threshold value defined as 10 mV ms^{-1}, which was also used to align APs for averaging. AP waveforms were isolated by our custom software (100 data points before AP onset to 150 data points past AP peak). First (dV/dt) and second (d^2V/dt^2) derivatives

Table 1. Epilepsy-associated proteins found in the AIS with a summary of their human epilepsy mutations and human phenotypes

Gene	Gene product	Mutations	Epilepsy syndrome(s)
SCN1A	Sodium channel α1 subunit	>100 known human mutations (for review see Reid *et al.* 2009; Stafstrom 2009*a*)	Dravet's syndrome, GEFS$^+$
SCN2A	Sodium channel α2 subunit	>10 mutations (for review see Reid *et al.* 2009)	BFNIS, encephalopathies
SCN8A	Sodium channel α6 subunit	P1719RfsX6 (Trudeau *et al.* 2006)	Epilepsy phenotype described to date only in mouse models
SCN1B	Sodium channel β1 subunit	C121W (Wallace *et al.* 1998) 5AA deletion (Audenaert *et al.* 2003) R85C/R85H (Scheffer *et al.* 2007) R125C (Patino *et al.* 2009)	GEFS$^+$
KCNQ2/3	Potassium channel (K_V7.2/3)	>50 mutations (for review see Reid *et al.* 2009)	BFNS
KCNA1	Potassium channel (K_V1.1)	>20 mutations (reviewed in Jen *et al.* 2007)	Partial epilepsy and episodic ataxia
CACNA1H	Calcium Channel (T-type, Ca_V3.2)	>30 mutations (Chen *et al.* 2003; Heron *et al.* 2004; Khosravani *et al.* 2004; Khosravani *et al.* 2005; Vitko *et al.* 2005; Heron *et al.* 2007; Powell *et al.* 2009; Reid *et al.* 2009)	IGE
GABRG2	$GABA_A$ receptor (γ2)	R43Q (Baulac *et al.* 2001; Wallace *et al.* 2001) K289M (Baulac *et al.* 2001) R139G (Audenaert *et al.* 2006) Q351X (Harkin *et al.* 2002) (For review see Kang & Macdonald, 2009.)	FS/GEFS$^+$
GABRA1	$GABA_A$ receptor (α1)	A322D (Krampfl *et al.* 2005)	IGE
GABRB3	$GABA_A$ receptor (β3)	P11S, S15F, G32R (Tanaka *et al.* 2008)	CAE
CNTNAP2	Contactin-associated protein-like 2 (CASPR2)	3709delG (Strauss *et al.* 2006)	Focal epilepsy

were calculated numerically. Figure 2 shows averages of 8–9 tonically fired APs per cell for $n = 13$ neurons.

Virus particles and stereotaxic injections. We generated adenoassociated virus (AAV) preparations (AAV1/2-EGFP-γ2(wild-type) and AAV1/2-EGFP-γ2(Q43); infectious titre 8×10^6 to 8×10^7 cells ml^{-1}) using helper plasmids encoding *cap1* and *cap2* at a ratio of 1:1. Transcription from all AAV constructs was controlled by a hybrid cytomegalovirus enhancer/chicken β-actin (CBA) promoter. P28 C57B/6 mice were anaesthetised using 1.5% isofluorane. Rectal body temperature was maintained at 36.0–36.5°C with a closed loop regulated heating pad (FHC, Bowdoinham, ME, USA). Stereotaxic injections were performed as previously described (Wimmer *et al.* 2004) at the following coordinates: DG and/or CA1: $X \pm 1.75$ mm, Y −2.2 mm, Z −1.8 and −1.0 mm. CA3: $X \pm 2.7$ mm, Y −2.2 mm, Z −1.5 mm. Somatosensory cortex: $X \pm 3.0$ mm, Y −0.5 mm, Z −1.0 mm. Injected mice were held for 12–15 days to allow time for viral expression.

Preparation of paraformaldehyde-fixed brain slices and staining methods. Animals were anaesthetised with a lethal dose of sodium pentobarbitone (40 mg kg^{-1}) and transcardially perfused with 0.1 M phosphate buffer (PB) followed by PB with 1% (specifically used for Na_V1.1, 1.2 and 1.6) or 4% paraformaldehyde. The brain was extracted, and either immersed in 30% sucrose, frozen and cut to 20 μm thickness with a freezing microtome (Na_V1.1, 1.2, 1.6 and γ2) or used to make coronal vibrating microtome sections of 50–100 μm thickness. The following antibodies were used: mouse anti-ankyrinG (Zymed; 1:500), rabbit anti-Na^+ channel subunits (Panα, Sigma, S6936, 1:500), Na_v1.1 (Clone K74/71, NeuroMab, Davis, CA, USA), Na_v1.2 (NeuroMab, Clone K69/3), Na_v1.6 (NeuroMab, Clone K87A/10) and rabbit anti-γ2 (1:300, ABcam, Cambridge, UK). Secondary antibodies were conjugated to Alexa dyes of different wavelengths (405, 488 or 594 nm; 1:300; Invitrogen).

Confocal laser scanning fluorescence microscopy and quantification of γ2 clusters. Confocal image stacks were acquired with an Olympus FV1000 confocal microscope, equipped with 405 nm, 473 nm and 559 nm diode lasers, using an Olympus 60× oil-immersion objective (NA 1.35). 3D image stacks were recorded considering Nyquist criteria. Stacks were deconvolved using Huygens Essential software (v. 2.31; Scientific Volume Imaging, Hilversum, The Netherlands).

$\gamma 2$ clusters in the AIS were quantified in tissue immunostained for AnkG and $\gamma 2$ using a workflow adapted from Wouterlood *et al.* (2008). In brief, an objective threshold for the $\gamma 2$ channel was generated using ImageJ (Abramoff *et al.* 2004) plugin '3D object counter' (written by Fabrice Cordelieres, Institut Curie, Orsay, France) in combination with a script detailed in Wouterlood *et al.* (2008); the AnkG channel was thresholded manually. Subsequently, regions of colocalisation between $\gamma 2$ and AnkG were extracted using the ImageJ plugin 'colocalisation highlighter' (created by Pierre Bourdoncle, Institut Jacques Monod, Service Imagerie, Paris) and exported as a separate channel ('$\gamma 2$/AnkG coloc'). This $\gamma 2$/AnkG coloc channel specifically identified $\gamma 2$ clusters localised in AISs. $\gamma 2$, AnkG and $\gamma 2$/AnkG coloc channels were then 3D reconstructed together and $\gamma 2$ clusters were quantified per 10 μm AIS length.

Statistical analyses. Data are presented as means ± S.E.M. Statistical analysis between two independent datasets was performed using Student's two-tailed unpaired *t* test using Prism 4.0 (GraphPad Software Inc., La Jolla, CA, USA). Where appropriate, data were tested for normal distribution using Kolmogorov–Smirnov normality test; if data distribution was not normal, non-parametric tests were used. For comparison of multiple datasets one-way ANOVA with Bonferroni's *post hoc* test was used.

References

Abramoff MD, Magelhaes PJ & Ram SJ (2004). Image processing with ImageJ. *Bioph Intern* **11**, 36–42.

Araki T & Otani T (1955). Response of single motoneurons to direct stimulation in toad's spinal cord. *J Neurophysiol* **18**, 472–485.

Audenaert D, Claes L, Ceulemans B, Lofgren A, Van Broeckhoven C & De Jonghe P (2003). A deletion in SCN1B is associated with febrile seizures and early-onset absence epilepsy. *Neurology* **61**, 854–856.

Audenaert D, Van Broeckhoven C & De Jonghe P (2006). Genes and loci involved in febrile seizures and related epilepsy syndromes. *Hum Mutat* **27**, 391–401.

Baulac S, Huberfeld G, Gourfinkel-An I, Mitropoulou G, Beranger A, Prud'homme JF, Baulac M, Brice A, Bruzzone R & LeGuern E (2001). First genetic evidence of $GABA_A$ receptor dysfunction in epilepsy: a mutation in the $\gamma 2$-subunit gene. *Nat Genet* **28**, 46–48.

Bender KJ & Trussell LO (2009). Axon initial segment Ca^{2+} channels influence action potential generation and timing. *Neuron* **61**, 259–271.

Berkovic SF, Heron SE, Giordano L, Marini C, Guerrini R, Kaplan RE, Gambardella A, Steinlein OK, Grinton BE, Dean JT, Bordo L, Hodgson BL, Yamamoto T, Mulley JC, Zara F & Scheffer IE (2004). Benign familial neonatal-infantile seizures: characterization of a new sodium channelopathy. *Ann Neurol* **55**, 550–557.

Bianchi MT, Song L, Zhang H & Macdonald RL (2002). Two different mechanisms of disinhibition produced by $GABA_A$ receptor mutations linked to epilepsy in humans. *J Neurosci* **22**, 5321–5327.

Blumenfeld H, Lampert A, Klein JP, Mission J, Chen MC, Rivera M, Dib-Hajj S, Brennan AR, Hains BC & Waxman SG (2009). Role of hippocampal sodium channel Nav1.6 in kindling epileptogenesis. *Epilepsia* **50**, 44–55.

Boiko T, Van Wart A, Caldwell JH, Levinson SR, Trimmer JS & Matthews G (2003). Functional specialization of the axon initial segment by isoform-specific sodium channel targeting. *J Neurosci* **23**, 2306–2313.

Bowser DN, Wagner DA, Czajkowski C, Cromer BA, Parker MW, Wallace RH, Harkin LA, Mulley JC, Marini C, Berkovic SF, Williams DA, Jones MV & Petrou S (2002). Altered kinetics and benzodiazepine sensitivity of a $GABA_A$ receptor subunit mutation [γ_2(R43Q)] found in human epilepsy. *Proc Natl Acad Sci U S A* **99**, 15170–15175.

Brackenbury WJ, Calhoun JD, Chen C, Miyazaki H, Nukina N, Oyama F, Ranscht B & Isom LL (2010). Functional reciprocity between Na^+ channel Nav1.6 and $\beta 1$ subunits in the coordinated regulation of excitability and neurite outgrowth. *Proc Natl Acad Sci U S A* **107**, 2283–2288.

Brew HM, Gittelman JX, Silverstein RS, Hanks TD, Demas VP, Robinson LC, Robbins CA, McKee-Johnson J, Chiu SY, Messing A & Tempel BL (2007). Seizures and reduced life span in mice lacking the potassium channel subunit Kv1.2, but hypoexcitability and enlarged Kv1 currents in auditory neurons. *J Neurophysiol* **98**, 1501–1525.

Browne DL, Gancher ST, Nutt JG, Brunt ER, Smith EA, Kramer P & Litt M (1994). Episodic ataxia/myokymia syndrome is associated with point mutations in the human potassium channel gene, KCNA1. *Nat Genet* **8**, 136–140.

Cardin JA, Carlen M, Meletis K, Knoblich U, Zhang F, Deisseroth K, Tsai LH & Moore CI (2009). Driving fast-spiking cells induces gamma rhythm and controls sensory responses. *Nature* **459**, 663–667.

Chen Y, Lu J, Pan H, Zhang Y, Wu H, Xu K, Liu X, Jiang Y, Bao X, Yao Z, Ding K, Lo WH, Qiang B, Chan P, Shen Y & Wu X (2003). Association between genetic variation of CACNA1H and childhood absence epilepsy. *Ann Neurol* **54**, 239–243.

Christie SB & De Blas AL (2003). GABAergic and glutamatergic axons innervate the axon initial segment and organize $GABA_A$ receptor clusters of cultured hippocampal pyramidal cells. *J Comp Neurol* **456**, 361–374.

Chung HJ, Jan YN & Jan LY (2006). Polarized axonal surface expression of neuronal KCNQ channels is mediated by multiple signals in the KCNQ2 and KCNQ3 C-terminal domains. *Proc Natl Acad Sci U S A* **103**, 8870–8875.

Coombs JS, Curtis DR & Eccles JC (1957). The generation of impulses in motoneurones. *J Physiol* **139**, 232–249.

Dodge FA & Cooley JW (1973). Action potential of the motoneuron. *IBM J Res Dev* **17**, 219–229.

Dube CM, Brewster AL, Richichi C, Zha Q & Baram TZ (2007). Fever, febrile seizures and epilepsy. *Trends Neurosci* **30**, 490–496.

Duflocq A, Le Bras B, Bullier E, Couraud F & Davenne M (2008). Nav1.1 is predominantly expressed in nodes of Ranvier and axon initial segments. *Mol Cell Neurosci* **39**, 180–192.

Fatt P (1957). Sequence of events in synaptic activation of a motoneurone. *J Neurophysiol* **20**, 61–80.

Ferreira MA, O'Donovan MC, Meng YA, Jones IR, Ruderfer DM, Jones L, Fan J, Kirov G, Perlis RH, Green EK, Smoller JW, Grozeva D, Stone J, Nikolov I, Chambert K, Hamshere ML, Nimgaonkar VL, Moskvina V, Thase ME, Caesar S, Sachs GS, Franklin J, Gordon-Smith K, Ardlie KG, Gabriel SB, Fraser C, Blumenstiel B, Defelice M, Breen G, Gill M, Morris DW, Elkin A, Muir WJ, McGhee KA, Williamson R, MacIntyre DJ, MacLean AW, St Clair D, Robinson M, Van Beck M, Pereira AC, Kandaswamy R, McQuillin A, Collier DA, Bass NJ, Young AH, Lawrence J, Ferrier IN, Anjorin A, Farmer A, Curtis D, Scolnick EM, McGuffin P, Daly MJ, Corvin AP, Holmans PA, Blackwood DH, Gurling HM, Owen MJ, Purcell SM, Sklar P & Craddock N (2008). Collaborative genome-wide association analysis supports a role for ANK3 and CACNA1C in bipolar disorder. *Nat Genet* **40**, 1056–1058.

Frugier G, Coussen F, Giraud MF, Odessa MF, Emerit MB, Boue-Grabot E & Garret M (2007). A γ2(R43Q) mutation, linked to epilepsy in humans, alters $GABA_A$ receptor assembly and modifies subunit composition on the cell surface. *J Biol Chem* **282**, 3819–3828.

Glickfeld LL, Roberts JD, Somogyi P & Scanziani M (2009). Interneurons hyperpolarize pyramidal cells along their entire somatodendritic axis. *Nat Neurosci* **12**, 21–23.

Goldberg EM, Clark BD, Zagha E, Nahmani M, Erisir A & Rudy B (2008). K^+ channels at the axon initial segment dampen near-threshold excitability of neocortical fast-spiking GABAergic interneurons. *Neuron* **58**, 387–400.

Goldschen-Ohm MP, Wagner DA, Petrou S & Jones MV (2010). An epilepsy-related region in the $GABA_A$ receptor mediates long-distance effects on GABA and benzodiazepine binding sites. *Mol Pharmacol* **77**, 35–45.

Harkin LA, Bowser DN, Dibbens LM, Singh R, Phillips F, Wallace RH, Richards MC, Williams DA, Mulley JC, Berkovic SF, Scheffer IE & Petrou S (2002). Truncation of the $GABA_A$-receptor γ2 subunit in a family with generalized epilepsy with febrile seizures plus. *Am J Hum Genet* **70**, 530–536.

Hedstrom KL, Xu X, Ogawa Y, Frischknecht R, Seidenbecher CI, Shrager P & Rasband MN (2007). Neurofascin assembles a specialized extracellular matrix at the axon initial segment. *J Cell Biol* **178**, 875–886.

Heron SE, Khosravani H, Varela D, Bladen C, Williams TC, Newman MR, Scheffer IE, Berkovic SF, Mulley JC & Zamponi GW (2007). Extended spectrum of idiopathic generalized epilepsies associated with CACNA1H functional variants. *Ann Neurol* **62**, 560–568.

Heron SE, Phillips HA, Mulley JC, Mazarib A, Neufeld MY, Berkovic SF & Scheffer IE (2004). Genetic variation of CACNA1H in idiopathic generalized epilepsy. *Ann Neurol* **55**, 595–596.

Hill AS, Nishino A, Nakajo K, Zhang G, Fineman JR, Selzer ME, Okamura Y & Cooper EC (2008). Ion channel clustering at the axon initial segment and node of Ranvier evolved sequentially in early chordates. *PLoS Genet* **4**, e1000317.

Howard A, Tamas G & Soltesz I (2005). Lighting the chandelier: new vistas for axo-axonic cells. *Trends Neurosci* **28**, 310–316.

Hu W, Tian C, Li T, Yang M, Hou H & Shu Y (2009). Distinct contributions of $Na_v1.6$ and $Na_v1.2$ in action potential initiation and backpropagation. *Nat Neurosci* **12**, 996–1002.

Inda MC, DeFelipe J & Munoz A (2006). Voltage-gated ion channels in the axon initial segment of human cortical pyramidal cells and their relationship with chandelier cells. *Proc Natl Acad Sci U S A* **103**, 2920–2925.

Jen JC, Graves TD, Hess EJ, Hanna MG, Griggs RC & Baloh RW (2007). Primary episodic ataxias: diagnosis, pathogenesis and treatment. *Brain* **130**, 2484–2493.

Jentsch TJ (2000). Neuronal KCNQ potassium channels: physiology and role in disease. *Nat Rev* **1**, 21–30.

Johnston J, Griffin SJ, Baker C, Skrzypiec A, Chernova T & Forsythe ID (2008). Initial segment Kv2.2 channels mediate a slow delayed rectifier and maintain high frequency action potential firing in medial nucleus of the trapezoid body neurons. *J Physiol* **586**, 3493–3509.

Kang JQ & Macdonald RL (2004). The $GABA_A$ receptor γ2 subunit R43Q mutation linked to childhood absence epilepsy and febrile seizures causes retention of $\alpha1\beta2\gamma2$S receptors in the endoplasmic reticulum. *J Neurosci* **24**, 8672–8677.

Kang JQ & Macdonald RL (2009). Making sense of nonsense $GABA_A$ receptor mutations associated with genetic epilepsies. *Trends Mol Med* **15**, 430–438.

Khirug S, Yamada J, Afzalov R, Voipio J, Khiroug L & Kaila K (2008). GABAergic depolarization of the axon initial segment in cortical principal neurons is caused by the Na-K-2Cl cotransporter NKCC1. *J Neurosci* **28**, 4635–4639.

Khosravani H, Altier C, Simms B, Hamming KS, Snutch TP, Mezeyova J, McRory JE & Zamponi GW (2004). Gating effects of mutations in the Cav3.2 T-type calcium channel associated with childhood absence epilepsy. *J Biol Chem* **279**, 9681–9684.

Khosravani H, Bladen C, Parker DB, Snutch TP, McRory JE & Zamponi GW (2005). Effects of Cav3.2 channel mutations linked to idiopathic generalized epilepsy. *Ann Neurol* **57**, 745–749.

Kole MH, Ilschner SU, Kampa BM, Williams SR, Ruben PC & Stuart GJ (2008). Action potential generation requires a high sodium channel density in the axon initial segment. *Nat Neurosci* **11**, 178–186.

Kole MH, Letzkus JJ & Stuart GJ (2007). Axon initial segment Kv1 channels control axonal action potential waveform and synaptic efficacy. *Neuron* **55**, 633–647.

Kostopoulos GK (2001). Involvement of the thalamocortical system in epileptic loss of consciousness. *Epilepsia* **42**(Suppl 3), 13–19.

Krampfl K, Maljevic S, Cossette P, Ziegler E, Rouleau GA, Lerche H & Bufler J (2005). Molecular analysis of the A322D mutation in the GABA receptor α-subunit causing juvenile myoclonic epilepsy. *Eur J Neurosci* **22**, 10–20.

Kress GJ, Dowling MJ, Eisenman LN & Mennerick S (2009). Axonal sodium channel distribution shapes the depolarized action potential threshold of dentate granule neurons. *Hippocampus* **20**, 558–571.

Lorincz A & Nusser Z (2008). Cell-type-dependent molecular composition of the axon initial segment. *J Neurosci* **28**, 14329–14340.

Martin MS, Tang B, Papale LA, Yu FH, Catterall WA & Escayg A (2007). The voltage-gated sodium channel Scn8a is a genetic modifier of severe myoclonic epilepsy of infancy. *Hum Mol Genet* **16**, 2892–2899.

Miceli F, Soldovieri MV, Lugli L, Bellini G, Ambrosino P, Migliore M, del Giudice EM, Ferrari F, Pascotto A & Taglialatela M (2009). Neutralization of a unique, negatively-charged residue in the voltage sensor of K_V 7.2 subunits in a sporadic case of benign familial neonatal seizures. *Neurobiol Dis* **34**, 501–510.

Molnar G, Olah S, Komlosi G, Fule M, Szabadics J, Varga C, Barzo P & Tamas G (2008). Complex events initiated by individual spikes in the human cerebral cortex. *PLoS Biol* **6**, e222.

Nusser Z, Roberts JD, Baude A, Richards JG, Sieghart W & Somogyi P (1995). Immunocytochemical localization of the α1 and β2/3 subunits of the $GABA_A$ receptor in relation to specific GABAergic synapses in the dentate gyrus. *Eu J Neurosci* **7**, 630–646.

Oakley JC, Kalume F, Yu FH, Scheuer T & Catterall WA (2009). Temperature- and age-dependent seizures in a mouse model of severe myoclonic epilepsy in infancy. *Proc Natl Acad Sci U S A* **106**, 3994–3999.

Ogawa Y & Rasband MN (2008). The functional organization and assembly of the axon initial segment. *Curr Opin Neurobiol* **18**, 307–313.

Ogiwara I, Ito K, Sawaishi Y, Osaka H, Mazaki E, Inoue I, Montal M, Hashikawa T, Shike T, Fujiwara T, Inoue Y, Kaneda M & Yamakawa K (2009). De novo mutations of voltage-gated sodium channel αII gene SCN2A in intractable epilepsies. *Neurology* **73**, 1046–1053.

Ogiwara I, Miyamoto H, Morita N, Atapour N, Mazaki E, Inoue I, Takeuchi T, Itohara S, Yanagawa Y, Obata K, Furuichi T, Hensch TK & Yamakawa K (2007). $Na_v1.1$ localizes to axons of parvalbumin-positive inhibitory interneurons: a circuit basis for epileptic seizures in mice carrying an Scn1a gene mutation. *J Neurosci* **27**, 5903–5914.

Palay SL, Sotelo C, Peters A & Orkand PM (1968). The axon hillock and the initial segment. *J Cell Biol* **38**, 193–201.

Palmer LM & Stuart GJ (2006). Site of action potential initiation in layer 5 pyramidal neurons. *J Neurosci* **26**, 1854–1863.

Papale LA, Beyer B, Jones JM, Sharkey LM, Tufik S, Epstein M, Letts VA, Meisler MH, Frankel WN & Escayg A (2009). Heterozygous mutations of the voltage-gated sodium channel SCN8A are associated with spike-wave discharges and absence epilepsy in mice. *Hum Mol Genet* **18**, 1633–1641.

Patino GA, Claes LR, Lopez-Santiago LF, Slat EA, Dondeti RS, Chen C, O'Malley HA, Gray CB, Miyazaki H, Nukina N, Oyama F, De Jonghe P & Isom LL (2009). A functional null mutation of SCN1B in a patient with Dravet syndrome. *J Neurosci* **29**, 10764–10778.

Powell KL, Cain SM, Ng C, Sirdesai S, David LS, Kyi M, Garcia E, Tyson JR, Reid CA, Bahlo M, Foote SJ, Snutch TP & O'Brien TJ (2009). A Cav3.2 T-type calcium channel point mutation has splice-variant-specific effects on function and segregates with seizure expression in a polygenic rat model of absence epilepsy. *J Neurosci* **29**, 371–380.

Reid CA, Berkovic SF & Petrou S (2009). Mechanisms of human inherited epilepsies. *Progr Neurobiol* **87**, 41–57.

Rosenbluth J (1976). Intramembranous particle distribution at the node of Ranvier and adjacent axolemma in myelinated axons of the frog brain. *J Neurocytol* **5**, 731–745.

Royeck M, Horstmann MT, Remy S, Reitze M, Yaari Y & Beck H (2008). Role of axonal $Na_V1.6$ sodium channels in action potential initiation of CA1 pyramidal neurons. *J Neurophysiol* **100**, 2361–2380.

Rush AM, Craner MJ, Kageyama T, Dib-Hajj SD, Waxman SG & Ranscht B (2005). Contactin regulates the current density and axonal expression of tetrodotoxin-resistant but not tetrodotoxin-sensitive sodium channels in DRG neurons. *Eur J Neurosci* **22**, 39–49.

Sarmiere PD, Weigle CM & Tamkun MM (2008). The Kv2.1 K^+ channel targets to the axon initial segment of hippocampal and cortical neurons in culture and in situ. *BMC Neurosci* **9**, 112.

Schafer DP, Jha S, Liu F, Akella T, McCullough LD & Rasband MN (2009). Disruption of the axon initial segment cytoskeleton is a new mechanism for neuronal injury. *J Neurosci* **29**, 13242–13254.

Scheffer IE, Harkin LA, Grinton BE, Dibbens LM, Turner SJ, Zielinski MA, Xu R, Jackson G, Adams J, Connellan M, Petrou S, Wellard RM, Briellmann RS, Wallace RH, Mulley JC & Berkovic SF (2007). Temporal lobe epilepsy and GEFS+ phenotypes associated with SCN1B mutations. *Brain* **130**, 100–109.

Scheffer IE, Zhang YH, Jansen FE & Dibbens L (2009). Dravet syndrome or genetic (generalized) epilepsy with febrile seizures plus? *Brain Dev* **31**, 394–400.

Shah MM, Migliore M, Valencia I, Cooper EC & Brown DA (2008). Functional significance of axonal Kv7 channels in hippocampal pyramidal neurons. *Proc Natl Acad Sci U S A* **105**, 7869–7874.

Singh NA, Pappas C, Dahle EJ, Claes LR, Pruess TH, De Jonghe P, Thompson J, Dixon M, Gurnett C, Peiffer A, White HS, Filloux F & Leppert MF (2009). A role of SCN9A in human epilepsies, as a cause of febrile seizures and as a potential modifier of Dravet syndrome. *PLoS Genet* **5**, e1000649.

Smart SL, Lopantsev V, Zhang CL, Robbins CA, Wang H, Chiu SY, Schwartzkroin PA, Messing A & Tempel BL (1998). Deletion of the $K_V1.1$ potassium channel causes epilepsy in mice. *Neuron* **20**, 809–819.

Song AH, Wang D, Chen G, Li Y, Luo J, Duan S & Poo MM (2009). A selective filter for cytoplasmic transport at the axon initial segment. *Cell* **136**, 1148–1160.

Stafstrom CE (2009*a*). Severe epilepsy syndromes of early childhood: the link between genetics and pathophysiology with a focus on SCN1A mutations. *J Child Neurol* **24**, 15S–23S.

Stafstrom CE (2009*b*). To depolarize or hyperpolarize? At the axon initial segment, E_{GABA} sets the stage. *Epilepsy Curr* **9**, 28–29.

Strauss KA, Puffenberger EG, Huentelman MJ, Gottlieb S, Dobrin SE, Parod JM, Stephan DA & Morton DH (2006). Recessive symptomatic focal epilepsy and mutant contactin-associated protein-like 2. *N Engl J Med* **354**, 1370–1377.

Szabadics J, Varga C, Molnar G, Olah S, Barzo P & Tamas G (2006). Excitatory effect of GABAergic axo-axonic cells in cortical microcircuits. *Science* **311**, 233–235.

Tan HO, Reid CA, Single FN, Davies PJ, Chiu C, Murphy S, Clarke AL, Dibbens L, Krestel H, Mulley JC, Jones MV, Seeburg PH, Sakmann B, Berkovic SF, Sprengel R & Petrou S (2007). Reduced cortical inhibition in a mouse model of familial childhood absence epilepsy. *Proc Natl Acad Sci U S A* **104**, 17536–17541.

Tanaka M, Olsen RW, Medina MT, Schwartz E, Alonso ME, Duron RM, Castro-Ortega R, Martinez-Juarez IE, Pascual-Castroviejo I, Machado-Salas J, Silva R, Bailey JN, Bai D, Ochoa A, Jara-Prado A, Pineda G, Macdonald RL & Delgado-Escueta AV (2008). Hyperglycosylation and reduced GABA currents of mutated GABRB3 polypeptide in remitting childhood absence epilepsy. *Am J Hum Genet* **82**, 1249–1261.

Thomas EA, Hawkins RJ, Richards KL, Xu R, Gazina EV & Petrou S (2009). Heat opens axon initial segment sodium channels: A febrile seizure mechanism? *Ann Neurol* **66**, 219–226.

Trudeau MM, Dalton JC, Day JW, Ranum LP & Meisler MH (2006). Heterozygosity for a protein truncation mutation of sodium channel SCN8A in a patient with cerebellar atrophy, ataxia, and mental retardation. *J Med Genet* **43**, 527–530.

Van Wart A, Trimmer JS & Matthews G (2007). Polarized distribution of ion channels within microdomains of the axon initial segment. *J Comp Neurol* **500**, 339–352.

Vitko I, Chen Y, Arias JM, Shen Y, Wu XR & Perez-Reyes E (2005). Functional characterization and neuronal modelling of the effects of childhood absence epilepsy variants of CACNA1H, a T-type calcium channel. *J Neurosci* **25**, 4844–4855.

Wallace RH, Marini C, Petrou S, Harkin LA, Bowser DN, Panchal RG, Williams DA, Sutherland GR, Mulley JC, Scheffer IE & Berkovic SF (2001). Mutant $GABA_A$ receptor γ2-subunit in childhood absence epilepsy and febrile seizures. *Nat Genet* **28**, 49–52.

Wallace RH, Wang DW, Singh R, Scheffer IE, George AL Jr, Phillips HA, Saar K, Reis A, Johnson EW, Sutherland GR, Berkovic SF & Mulley JC (1998). Febrile seizures and generalized epilepsy associated with a mutation in the Na^+-channel β1 subunit gene SCN1B. *Nat Genet* **19**, 366–370.

Waxman SG & Quick DC (1978). Intra-axonal ferric ion-ferrocyanide staining of nodes of Ranvier and initial segments in central myelinated fibres. *Brain Res* **144**, 1–10.

Wimmer VC, Nevian T & Kuner T (2004). Targeted in vivo expression of proteins in the calyx of Held. *Pflugers Arch* **449**, 319–333.

Winkels R, Jedlicka P, Weise FK, Schultz C, Deller T & Schwarzacher SW (2009). Reduced excitability in the dentate gyrus network of βIV-spectrin mutant mice in vivo. *Hippocampus* **19**, 677–686.

Wouterlood FG, Boekel AJ, Kajiwara R & Belien JA (2008). Counting contacts between neurons in 3D in confocal laser scanning images. *J Neurosci Methods* **171**, 296–308.

Xu R, Thomas EA, Jenkins M, Gazina EV, Chiu C, Heron SE, Mulley JC, Scheffer IE, Berkovic SF & Petrou S (2007). A childhood epilepsy mutation reveals a role for developmentally regulated splicing of a sodium channel. *Mol Cell Neurosci* **35**, 292–301.

Yu FH, Mantegazza M, Westenbroek RE, Robbins CA, Kalume F, Burton KA, Spain WJ, McKnight GS, Scheuer T & Catterall WA (2006). Reduced sodium current in GABAergic interneurons in a mouse model of severe myoclonic epilepsy in infancy. *Nat Neurosci* **9**, 1142–1149.

Author contributions

V.C.W., C.A.R. and E.Y.S. did the experiments at the Howard Florey Institute, V.C.W. and C.A.R. analysed the data, and V.C.W., C.A.R., S.F.B. and S.P. wrote the manuscript.